



Nonnegative unmixing methodology applied on Brillouin Optical Fiber Sensor

Edouard Buchoud, Valeriu Vrabie, Jerome I. Mars, Alexandre Girard, Guy d'Urso, Sylvain Blairon, Jean-Marie Henault

► To cite this version:

Edouard Buchoud, Valeriu Vrabie, Jerome I. Mars, Alexandre Girard, Guy d'Urso, et al.. Nonnegative unmixing methodology applied on Brillouin Optical Fiber Sensor. EUSIPCO 2013 - 21th European Signal Processing Conference, Sep 2013, Marrakech, Morocco. pp.1569739197. hal-00986252

HAL Id: hal-00986252

<https://hal.science/hal-00986252>

Submitted on 1 May 2014

HAL is a multi-disciplinary open access archive for the deposit and dissemination of scientific research documents, whether they are published or not. The documents may come from teaching and research institutions in France or abroad, or from public or private research centers.

L'archive ouverte pluridisciplinaire **HAL**, est destinée au dépôt et à la diffusion de documents scientifiques de niveau recherche, publiés ou non, émanant des établissements d'enseignement et de recherche français ou étrangers, des laboratoires publics ou privés.

NONNEGATIVE UNMIXING METHODOLOGY APPLIED ON BRILLOUIN OPTICAL FIBER SENSOR

Edouard Buchoud^{1,3}, Valeriu Vrabie², Jerome Mars¹, Alexandre Girard³, Guy D'Urso³, Sylvain Blairon³, Jean-Marie Henault³

¹GIPSA-LAB, Grenoble France, ²CRESTIC, Reims France, ³EDF R&D, Chatou France

ABSTRACT

As a complement to conventional sensors, Distributed Optical Fiber Sensors (DOFS) have gradually played a prominent role in Structural Health Monitoring (SHM) for the last decade. The distributed Brillouin sensor enables to measure strain along kilometers of cable with a spatial resolution of 1 meter. The challenge is to have a centimeter spatial resolution to improve structure defaults detection and localization. A numerical model, based on the sensor physic, is first proposed in order to study Brillouin spectra distortion depending on strain distribution within spatial resolution. Then, based on nonnegative least squares (NNLS) problem, Brillouin spectra are decomposed into several elementary spectra. The estimated central frequencies and maxima permit to estimate a centimeter frequency distribution within the spatial resolution. It has been verified with numerical and experimental data: that method enables to enhance the accuracy and spatial resolution of the sensor from meter to centimeter.

Index Terms— NonNegative Matrix Factorization, NonNegative Least Square (NNLS) problem, spatial resolution enhancement, B-OTDA, Optical Backscatter Reflectometer, Structural Health Monitoring

1. INTRODUCTION

Durability of civil infrastructures is a crucial issue that can have major economical, social and environmental impacts. Infrastructure owners must face difficult challenges, such as optimization of maintenance and extension of service life. In this context, Structural Health Monitoring (SHM) is considered as a key procedure of industrial process, because it enables a real-time diagnosis of the state of wear/damage of an infrastructure. In complementary to traditional sensors, distributed fiber optic sensors (DOFS) are an attractive tool for SHM [1]. The distributed Brillouin sensor (DBS), in comparison with other fiber optic sensors, has the advantage of combining distributed temperature and strain measurements over few meters to kilometers.

Several sensors are based on the Brillouin spectrum dependence on the temperature and strain into the optical fiber [2]. The article will focus on the functioning of an

industrialized Brillouin Optical Time Domain Analyzer (B-OTDA). Estimation of strain into the optical fiber is based on the determination of Brillouin frequency, defined as the abscissa of the maximum of Brillouin spectrum and calculated by fitting Lorentzian or pseudo-Voigt curves [3]. The Brillouin spectrum is measured for a spatial base integration of one meter of the optical fiber and a sampling of 40cm. Several studies are summarized in [4], based on optic physic theory and on signal processing schemes [7]. The last method enables to quantify some strain defects on optical fiber but there is a lack of accuracy on its location. However, for our application, the determination of a precise strain profile is a prior. For that purpose, our article presents a new signal processing approach based on Nonnegative unmixing methodology.

When local and substantial loads are applied on the optical fiber, several studies [5][6] showed that Brillouin spectrum is distorted. Peak frequency measurement obtained by the curves fitting technique gives only the global strain measurement. Indeed, in that case, Brillouin spectrum is asymmetric and broadening and can also have subpeaks. Information about local strain can be extracted from it. The aim of the article is to improve spatial resolution and strain accuracy.

The proposed article introduces a numerical model to model the industrialized B-OTDA device. It enables to study Brillouin spectrum distortion depending on strain distribution types. An unmixing methodology, based on NonNegative Least Square (NNLS) algorithm, is proposed to unmix Brillouin spectra into several elementary spectra. Their frequencies and maxima are linked with frequency distribution within the spatial resolution. A methodology enables to retrieve a precise Brillouin frequency profile depending on distance. This methodology is tested by numerical and experimental data.

2. BRILLOUIN SPECTRUM ACQUISITION

B-OTDA device launches two counter propagative lightwaves into an optical fiber. An energy transfer, called Brillouin gain, occurs when the two encounter, which is amplified by the sensing medium. One of the lightwaves has a fixed frequency, whereas the other is frequency-modulated.

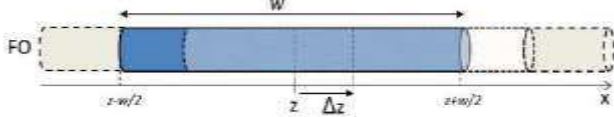


Figure 1: Representation of the spatial redundancy into the optical fiber.

The maximum energy transfer occurs when the difference between the two frequencies is exactly equal to the Brillouin frequency ν_B in the optical fiber, which is linearly dependent on the temperature and strain into the optical fiber [2]. The distributed character of such a sensor is achieved by time-resolved measurements. The spatial resolution w is defined by the length of lightwave impulsion; a 10ns impulsion gives a 1m spatial resolution. The impulsion is moving into the optical fiber; therefore we have several measurements depending on the length of the sensing medium as seen in Figure 1. With those parameters, it can interrogate kilometers of fiber. z is the center of the spatial resolution. All along the sensing medium, the spatial resolution is shifted by Δz to another zone of the optical fiber. So, there is spatial redundancy between several spectra. z is defined as $z = z_0 + k \cdot \Delta z$ in (3) with $k = 1, \dots, Nd$. Nd is the number of measured spectra into the optical fiber and is calculated as $Nd = (L - w) / \Delta z$ with L , the sensing length of the optical fiber. For each z , the Brillouin gain is acquired depending on the frequency difference of the two lightwaves, ν . Therefore, the raw data of the device is a matrix $G(\nu, z)$. Estimation of strain into the optical fiber is based on the determination of Brillouin frequency, defined as the abscissa of the maximum of Brillouin spectrum and calculated by fitting Lorentzian or pseudo-Voigt curves [3]. The relationship of Brillouin frequency shift between two states (a reference state R and a stressed state N) of the sensing medium, with the strain $\Delta \varepsilon$ and temperature ΔT changes are expressed as [2]:

$$\nu_{BA}(z) = \nu_{BR}(z) + C_T \Delta T(z) + C_\varepsilon \Delta \varepsilon(z) \quad (1)$$

where C_T and C_ε are the temperature and strain proportionally coefficients. $\nu_{BR}(z)$ is the Brillouin frequency at the reference state depending on distance z . This article is focused on strain changes into the optical fiber, therefore, ΔT is considered negligible.

3. MODEL DESCRIPTION

The present work focuses on the formulation of a model which can fit the industrialized B-OTDA behavior. F. Ravet [6] presented a model taking into account optical parameters which are involved into the experimental device. The presented model is related to the industrialized device. In every part of the optical fiber, a natural Brillouin spectrum exists $S_N(\nu)$. It has a Lorentzian shape [3] and is centered on the local Brillouin frequency, noted $\nu_B(x)$. Several studies showed that optical parameters disturbed natural Brillouin

spectrum shape [3]. In other words, the device has a transfer function $f(\nu)$, which modifies Brillouin spectrum shape. The convolution between $S_N(\nu)$ and the transfer function of the device is an elementary Brillouin spectrum, $S_e(\nu)$ expressed as:

$$S_e(\nu) = S_N(\nu) * f(\nu) \quad (2)$$

For a fixed z , the numerical Brillouin spectrum $G(\nu, z)$, within the spatial resolution, w , is modeled as the integral of all the elementary spectra $S_e(\nu)$ centered in the local Brillouin frequencies :

$$\tilde{G}(\nu, z) = \int_{z-w/2}^{z+w/2} S_e(\nu - \nu_B(x)) dx \quad (3)$$

where x is the curvilinear abscissa of the fiber. The problem can be reformulated as the convolution of $S_e(\nu)$ with the sum of Dirac function centered in $\nu_B(x)$. $S_e(\nu)$, depending on optical parameters and the optical fiber properties used, is found experimentally. Indeed, if the frequency distribution is uniform within w then the shape of $\tilde{G}(\nu, z)$ is equal to the shape of $S_e(\nu)$.

4. NUMERICAL SPECTRUM DISTORTION DEPENDING ON STRAIN DISTRIBUTION

In experimental conditions, studies [5][6] showed that strain variation are smoothed (and thus Brillouin frequencies profile) within the spatial resolution w . A very local strain variation within w leads to a non uniform frequency distribution and a Brillouin spectrum distortion: it is broadening and asymmetric.

Thanks to the model, the proposed numerical frequency profile shown in Figure 2.a. generates numerical Brillouin matrix shown in Figure 2.b. It presents distorted spectra, between $z = 4\text{m}$ and $z = 6\text{m}$, where the frequency profile presents high variations within w . The frequency is evolving from 10.93 GHz to 10.71 GHz in less than 2m. As observed in Figure 2.b., at $z = 5.4\text{m}$, the spectrum is highly distorted. Splitting w into several segments, considering a segment δx among w , we suppose that $\nu_B(x)$ is constant within δx and equal to ν_{Bj} . N is the number of segments as $N = w / \delta x$. This remains to discrete the integral in Eq. 3. As several segments can have the same ν_{Bj} , we can rewrite it as:

$$\tilde{G}(\nu, z) \cong \delta x \cdot \sum_{j=1}^P a_j \cdot S_e(\nu - \nu_{Bj}) \quad (4)$$

where, $S_e(\nu - \nu_{Bj})$ is the spectral component contained in the distorted spectrum, centered in ν_{Bj} , P is their number. The more the spectrum is broadening, the more P increases. For one spectral component m , a_m is the amplitude of the spectral component. It can be linked to the number of segments into w , noted \tilde{d}_m , with the same ν_{Bm} :

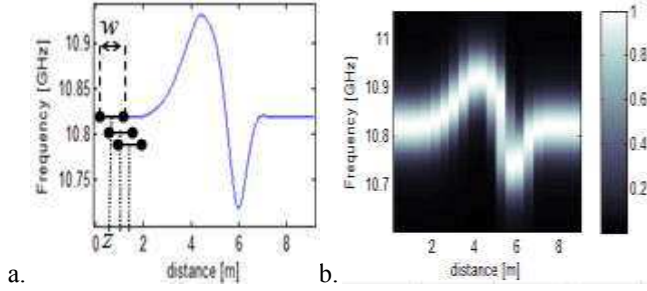


Figure 2: a. Smoothed frequency profile depending on Brillouin frequency (GHz) and distance (m). b. Corresponding numerical matrix $G(v,z)$ depending on frequency (GHz) and distance (m). The color scale is relative to the gain.

$$\tilde{d}_m = \frac{a_m}{\sum_{j=1}^P a_j} \cdot w \quad (5)$$

\tilde{d}_m is considered as a distance of w where the optical fiber is similarly stressed. However, the spatial information of the layout of the strain is not conserved. Therefore, the goal of the article is to estimate characteristics of the spectral components: $(a_j, v_{Bj})_z$; and then to estimate the frequency profile with a better spatial resolution.

5. NONNEGATIVE DECOMPOSITION OF BRILLOUIN SPECTRUM

The aim of the method is to find maxima and frequencies associated in order to find the frequency distribution within the spatial resolution. Several unmixing techniques exist but one property of the Brillouin spectrum is its positivity. Therefore methods like nonnegative matching pursuit [9], Nonnegative Matrix Factorization (NMF) [10], and Non Negative Least Square (NNLS) [11] can be used. The first two methods need a stopping criterion and the uniqueness of solutions has to be discussed. NMF estimates both mixing matrix and sources, while we need to estimate only the mixing matrix. NNLS is solved iteratively, and as shown by [11], convergence is respected. In our application, as proved in last paragraph, the form of the sources is known, which is the elementary Brillouin spectrum $S_e(v)$.

Thanks to NNLS, the problem is formulated as: given a matrix $E \in R^{N \times M}$, the set of observed values given by $\mathbf{g} \in R^N$, find a non negative vector $\mathbf{a} \in R^M$ to minimize:

$$\|E\mathbf{a} - \mathbf{g}\|_2^2 \quad (6)$$

where \mathbf{g} is a column of the measured Brillouin matrix $G(v,z)$ at a fixed distance z , the matrix E is a dictionary constructed by shifted versions of the elementary spectrum $S_e(v)$ and \mathbf{a} represents the corresponding weight vector.

The m^{th} column of the matrix E is:

$$E(v,m) = S_e(v) * \delta(v - m\Delta v) \quad (7)$$

the Δv is the frequency shift to be chosen, N is related to the frequency sampling of the B-OTDA device and M represents the number of shifted versions of the elementary spectrum. It means that we defined M possible spectral components. The smaller the frequency shift Δv , the more accurate the estimation of a spectrum will be.

The chosen algorithm enables to estimate the vector \mathbf{a} depending on the dictionary E . It optimizes the number of non null values P among the M possibilities. As we work on normalized spectra, if the strain is uniform within w , P will be equal to 1 and $a=1$. Then the more the spectrum is distorted, the more P increases.

It is repeated for each k^{th} measured Brillouin spectrum. Therefore, the result is a matrix $A \in R^{M \times Nd}$ containing the weight vectors \mathbf{a} for all the distances $z = z_0 + k \cdot \Delta z$.

6. ESTIMATION OF A FREQUENCY PROFILE

Here, a method is proposed to organize the local frequencies within w . The first main key is to use the spatial redundancy property. Several spectra are linked with the same portion of the optical fiber as shown in Figure 1. Therefore, for three adjacent positions $z_{i-1} = z_0 + (i-1) \cdot \Delta z$, $z_i = z_0 + i \cdot \Delta z$ and $z_{i+1} = z_0 + (i+1) \cdot \Delta z$, the means of the frequencies of each positions are compared, noted \bar{v}_B . It enables to find a global behavior of the frequency distribution. From those behaviors, we defined local variation within w as shown in Tab. 1.

Taking three adjacent spectra $G(v, z_{i-1})$, $G(v, z_i)$ and $G(v, z_{i+1})$, the NNLS algorithm estimate amplitudes and frequencies of the spectral components as shown in Fig. 3.a-c. The comparison of \bar{v}_{Bi} in this example leads to the fourth scenario. It means that there is a local maximum in w_i . The hypothesis is made that the local frequencies increase within w_{i-1} , respectively, decrease within w_{i+1} . Within w_i , the maximum of v_{Bi} is put on the center and the left frequencies are order depending on the adjacent tendencies. This layout is shown in Fig. 3.d. This process is repeated on each w . As there is spatial redundancy, for one fixed segment of w , superposition of several frequencies may appear. Thus, the mean of those frequencies contained in a sliding window noted Δx is calculated. Therefore, we estimate a new Brillouin frequency profile depending on the new spatial sampling Δx as shown in Fig. 3.e.

Cases	Comparison	Global	Local
1	$\bar{v}_{Bi-1} < \bar{v}_{Bi} < \bar{v}_{Bi+1}$	↗	-
2	$\bar{v}_{Bi-1} > \bar{v}_{Bi} > \bar{v}_{Bi+1}$	↘	-
3	$\bar{v}_{Bi} > \bar{v}_{Bi-1} > \bar{v}_{Bi+1}$	↗	Maxima
4	$\bar{v}_{Bi} > \bar{v}_{Bi+1} > \bar{v}_{Bi-1}$	↘	Minima
5	$\bar{v}_{Bi-1} > \bar{v}_{Bi+1} > \bar{v}_{Bi}$	↗	Minima
6	$\bar{v}_{Bi+1} > \bar{v}_{Bi-1} > \bar{v}_{Bi}$	↘	Maxima

Tab. 1. Six scenarii defining the local tendencies of the frequencies contained into three adjacent integration bases: w_{i-1} , w_i , and w_{i+1} .

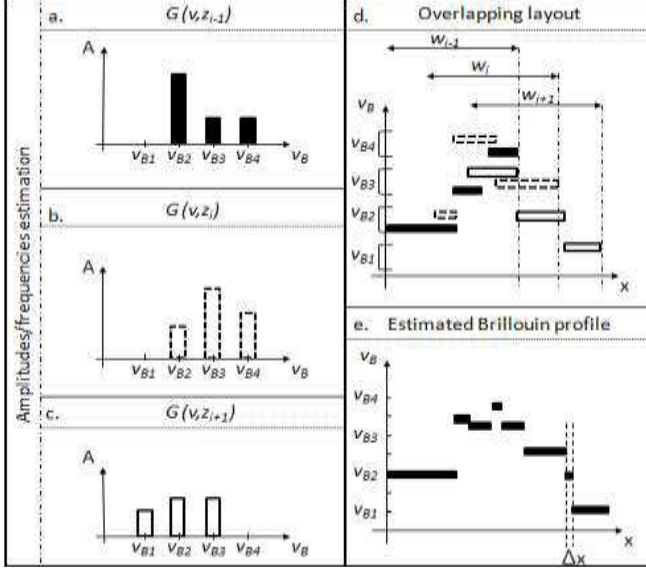


Figure 3: a-c: Result of the estimation of the characteristics of three adjacent spectra measured in z_{i-1} , z_i , and z_{i+1} . d. Layout of the frequencies within the w_i . e. Estimation of the Brillouin frequencies profile depending on the new spatial sampling Δx .

7. APPLICATION ON NUMERICAL DATA

The proposed methodology has been tested on the numerical matrix shown in Figure 2.b. A sources dictionary E is constructed with a pseudo-Voigt elementary Brillouin spectrum $S_e(v)$ shifted by $\Delta v = 10$ Hz, shown in Figure 4.a. For one spectrum, the NNLS algorithm finds the corresponding weight vector of each elementary spectrum as shown in Figure 4.b. for the example of the Brillouin spectrum acquired in $z = 4.4$ m. It is obvious that P is maximum where the spectrum is the more distorted. For the Brillouin spectra matrix $G(v, z)$, a corresponding weight matrix A shown in Figure 4.c.

The estimated weights are coherent with the input frequency profile (Figure 2.a): it found the right frequency where the frequency distribution is constant within w ; the maximum frequency found is 10.93 GHz and the minimum is 10.71 GHz. The resulting estimated frequency profile using the method proposed in section 6 is plotted in Figure 4.d with a chosen spatial sampling $\Delta x = 1$ cm.

It is compared with a profile estimated by an industrial B-OTDA device (crossed continuous line) and the input profile shown in Figure 2.b. Our estimation and the input are mixed up, whereas the bias is higher for B-OTDA profile where strain variations are important within w . If Δx is chosen greater, some strain variations won't be detected and localized. To authors' knowledge, it is the first time that a profile is given with such frequency accuracy and spatial resolution, from Brillouin spectra. Previous work [7] enables to detect and estimate some local strain but couldn't give such precise profile.

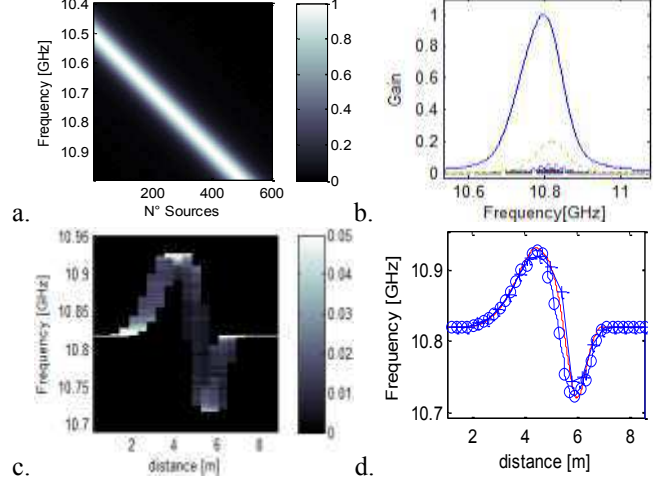


Figure 4: a. Dictionary of sources centered in local Brillouin frequencies in GHz. b. A distorted Brillouin spectrum (continuous line) and the associated estimated elementary spectra (dotted lines) for $z = 4.4$ m. c. Estimated weights matrix. d. Estimated profile (blue circle line) with $\Delta x = 1$ cm, reference profile (red continuous line) and measured by B-OTDA device (blue crossed line).

8. APPLICATION ON EXPERIMENTAL DATA

A controlled laboratory experiment has been carried out in order to validate our methodology. In a controlled temperature atmosphere, an optical fiber cable has been installed. The experimental bench enables to pull the cable constantly between two fixed points (10.5 m and 14 m). For each device, two measurements are made: when the cable is relaxed; then when it is pulled.

An Optical Backscatter Reflectometer (OBR) was used to measure the relative frequency shift between the two states of the cable with a spatial resolution of 1 centimeter [8]. Thanks to (1), the calculated strain, considered as the strain reference, is shown in Figure 5.a. and Figure 5.b. as the solid red curve. We can observe two important strain variations, around $2000 \mu\text{m/m}$ within few centimeters where the cable was fixed. An industrialized B-OTDA device was used to measure two Brillouin spectra matrices for each state of the cable. The parameters of this device are: $w = 1$ m and $\Delta z = 40$ cm. From Brillouin spectra, the device estimates Brillouin frequency profiles. The strain is calculated thanks to (1) and plotted (stars) in Figure 4.a. Comparing with the reference strain, where the strain variations are important within w , the strain estimated by the B-OTDA is not enough precise.

As strain variations are important, Brillouin spectra $G(v, z_1)$ and $G(v, z_2)$ are distorted due to integration of several shifted elementary spectra within w . First of all, the elementary spectrum $S_e(v)$ is estimated where the strain distribution into the optical fiber is constant.

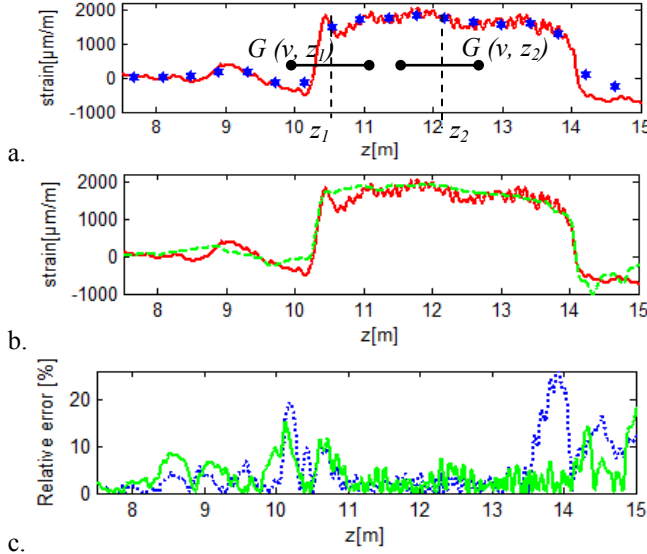


Figure 5: OBR strain measurement (red continuous line) and: a. B-OTDA interpolated strain measurement (blue points): $w=1\text{m}$, $\Delta z=40\text{cm}$. b. Estimated strain profile by the proposed method (dotted line) with $\Delta x=1\text{cm}$. c. Relative errors in percents between OBR: and interpolated B-OTDA strain profile (dotted line); and estimated one (continuous line)

Then, the presented algorithm decomposes each Brillouin spectrum using a dictionary matrix E . To construct this matrix, the frequency shift chosen is $\Delta\nu=1\text{MHz}$, and the new spatial sampling chosen is $\Delta x=1\text{cm}$. Thanks to our methodology, two frequency profiles are estimated. Using relation (1), the strain can be estimated and shown in Figure 5.b. As observed, the spatial resolution has been enhanced from 1m to 1cm .

The relative errors are calculated as L_2 norm between a strain reference: the OBR strain profile; and the two methodologies: the device strain profile and our estimated profile. They are plotted in Figure 5.c. The device strain profile has been interpolated in the purpose of comparison. It enables to observe that a second crucial point has been verified: the strain accuracy of the sensor has been improved where the strain distribution is not uniform within w . Thanks to that experiment, the model has been verified and the methodology validated.

9. CONCLUSION

The proposed article introduces a direct model of a B-OTDA device in order to study the Brillouin spectrum distortion when the strain distribution within the spatial resolution is non uniform. The proposed unmixing methodology enables to estimate amplitudes and local Brillouin frequencies of spectral components contained in distorted spectra. This approach is based on NNLS algorithm. A simple but novelty approach in this domain is the organization of estimated Brillouin local frequencies

within the spatial resolution. This approach enables to improve the accuracy of the sensor and its spatial resolution. Simulated and experimental data has validated this methodology. However, it merits further investigations in order to decrease estimation errors. In further works, others method will be tested as an inversion approach based on the proposed numerical model of the device.

10. REFERENCES

- [1] V. Lanticq, R. Gabet, F. Taillade and S. Delepine-Lesoille, "Distributed optical fibre sensors for Structural Health Monitoring: Upcoming challenges", *Optical Fiber, New developments*, Chapter 9, 2009.
- [2] X. Bao, J. Dhiwayo, N. Heron, D.J. Webb, and D.A. Jackson, "Experimental and theoretical studies on a distributed temperature sensor based on Brillouin scattering," *Journal of Lightwave Technology*, Vol. 13, No.7, pp. 1340-1348, 1995.
- [3] X. Bao, A. Brown, M. DeMerchant, and J. Smith, "Characterization of the Brillouin-loss Spectrum of Single-mode Fibers by Use of Very Short ($<10\text{ns}$) Pulses", *Optics Letters*, Vol. 23, No. 8, pp. 510-512, April 15, 1999.
- [4] X. Bao, and L. Chen, "Recent Progress in Brillouin Scattering Based Fiber Sensors", *Sensors*, Vol. 11, pp. 4152-4187, April 2011
- [5] F. Ravet, X. Bao, T. Ozbakkaloglu, and M. Saatcioglu, "Signature of structure failure using asymmetric and broadening factors of Brillouin spectrum", *IEEE photonics technology letters*, Vol. 18, No. 2, January 15, 2006.
- [6] E. Buchoud, S. Blairon, G. D'Urso, J-M. Henault, A. Girard, J. Mars, and V. Vrabie, "Detection of ground movement using the shape of Brillouin spectrum", *Near Surface Geoscience 2012*, Paris, France, September 5, 2012.
- [7] F. Ravet, X. Bao, Y. Li, Q. Yu, A. Yale, V.P. Kalosha, and L. Chen, "Signal processing technique for distributed Brillouin sensing at centimeter spatial resolution", *Journal of Lightwave Technology*, Vol. 25, No. 11, pp. 3610-3618, November 2007.
- [8] E. Buchoud, J. Mars, V. Vrabie, J-M. Henault, S. Blairon, A. Girard and G. D'Urso, "Development of an automatic algorithm to analyze the cracks evolution in a reinforced concrete structure from strain measurements performed by an Optical Backscatter Reflectometer", Workshop CSHM-4, Berlin, Germany November 6-8 2012.
- [9] S.G. Mallat and Z. Zhang, "Matching pursuits with time-frequency dictionaries", *IEEE Transactions on Signal Processing*, Vol. 41, No. 12, pp. 3397-3415, December 1993.
- [10] D.D. Lee and H.S. Seung, "Algorithm for non-negative matrix factorization", *Advances in neural information processing systems*, vol. 13, pp. 556-562, 2001.
- [11] Lawson, C.L. and R.J. Hanson, "Solving Least Squares Problems", *Prentice-Hall*, Chapter 23, p. 161, 1974.